AIChE

Photodecomposition of Organic Phosphorus in Aquatic Solution under Solar Irradiation with Nitrate: Kinetics and Influencing Water Parameters

Xiaolu Li,[a] Shaobo Yuan,[a] Yiyong Zhou,[b] Guanglong Liu,[a,b] and Duanwei Zhu[a]

[a]Lab of Eco-Environmental Engineering Research, College of Resources & Environment, Huazhong Agriculture University, Wuhan 430070, China

[b]Institute of Hydrobiology, the Chinese Academy of Sciences, Wuhan 430072, China; liugl@mail.hzau.edu.cn (for correspondence)

Published online 15 September 2016 in Wiley Online Library (wileyonlinelibrary.com). DOI 10.1002/ep.12471

The transformation of organic phosphorus plays an important role in the phosphorus cycle in the natural environment. In this study, a series of laboratory-based experiments were conducted to address the influence of nitrate (NO_3^-) photochemical activity on the transformation of methyl parathion under solar irradiation. It is demonstrated that the photodecomposition of methyl parathion by NO_3^- obeys pseudo-first-order reaction kinetics, with the photodecomposition rate increasing with NO_3^- concentration. The photodecomposition rates of methyl parathion by NO_3^- were strongly influenced by pH, concentration of humic acid and Fe^{3+}. Higher concentrations of Fe^{3+} and lower concentrations of humic acid accelerated the photodegradation induced by NO_3^-. Moreover, compared to alkaline media the acidic media can enhance the rate of methyl parathion degradation. Formation of the hydroxyl radical (•OH) was identified through the measurement of photoluminescence spectra (PL) using terephthalic acid as the trapping molecule. The primary transformation pathways of methyl parathion in the presence of NO_3^- under solar irradiation were proposed through the qualitative and quantitative analysis of byproducts. Intermediates, such as paraoxon, 4-nitrophenol and orthophosphate, were identified, and a mineralization pathway from methyl parathion to orthophosphate was proposed. © 2016 American Institute of Chemical Engineers Environ Prog, 36: 404–411, 2017

Keywords: kinetics, phosphorous, solar energy, eutrophication

INTRODUCTION

Phosphorus (P) is an essential element for living cells as a constituent of genetic materials, as well as energy-producing and cellular compounds [1]. In some aquatic ecosystems, the increased concentration of P in the water column has been considered as the primary factor responsible for accelerated eutrophication, by regulating the biogeochemical cycling of carbon, nutrients and other bioactive trace elements in the water column [2]. As a major component of the phosphorus in the aquatic environment, organic phosphorus plays an important role in the phosphorus cycle [3,4]. Previous studies revealed that the transformation of organic phosphorus in the natural environment could be an important source of water column phosphorus and a dynamic mechanism may be involved in the transformation of organic phosphorus [5,6]. However, little is known about this mechanism.

Phosphorus occurs naturally in aquatic environments in both inorganic and organic forms. Inorganic phosphorus is the most bioavailable P form and researchers pay more attention to its abundance, transformation and the impact on lake eutrophication [7–11]. However, the organic phosphorus also influences the aquatic environment [12]. In the last decade, the decomposition of organic phosphorus has been widely of concern [13,14]. Previous studies revealed that biotic and abiotic degradation are the primary pathways for the transformation of organic phosphorus in the environment [15]. The transformation of organic phosphorus to phosphate could maintain a low magnitude, long-term release of P in the water environment. Recent studies have demonstrated that phosphate could be released when the organic phosphorus is exposed to simulated solar irradiation with a photosensitizer [16,17]. However, other reports showed that organic phosphorus could be photodegraded, but the extent of degradation was dependent on the light sources and solution composition [18,19].

Nitrate ions are widely present in natural surface waters at concentrations classically in the 10^{-5} to 10^{-3} M range [20].In the past, nitrate was believed to only take part in biological cycles, but its photochemical activity has become evident in the last two decades [21].Nitrate photolysis produces reactive oxygen species according to reactions (1) and (2) [21–24]; the •OH radicals released could oxidize various organic substances [25,26]. Considerable concern was focused on the influence of nitrate photochemical activity on the organic substances' environmental behavior under solar irradiation because of its wide existence in natural water [27–29].

$$NO_3^- + h\nu \cdot NO_2 + O^- \quad (1)$$

$$O^- + H_2O \cdot OH + OH^- \quad (2)$$

The photochemistry of Fe(III)–oxalate complexes had been studied since the 1950s [15].

In the present study, methyl parathion, an organophosphate herbicide widely used in various parts of the world [30–32], was employed as target organic phosphorus and a series of laboratory-based experiments were conducted to address the influence of NO_3^- photochemical activity on photodecomposition of organic phosphorus compounds under solar irradiation. Kinetic studies were carried out in detail to explore its reactivity and the effects of environmental parameters and through the qualitative and quantitative analysis of byproducts, the transformation pathways of methyl parathion in the presence of NO_3^- under solar irradiation are proposed.

EXPERIMENTAL

Chemicals

The following reagents were used: methyl parathion (SP grade), and terephthalic acid (AR grade) were purchased from Sigma-Aldrich (U.S.). Suwanee River humic acids (HA) were purchased from the IHSS (International Humic Substances Society). $NaNO_3$ (AR grade), NaOH (AR grade), HCl (AR grade) and $FeCl_3$ (AR grade, >30%) were supplied by Guoyao Chemical Co. (Shanghai, China). All the chemicals were used without further purification and all solutions were prepared with deionized water from a Millipore device (Milli-Q) in the experiments.

Experimental Setups and Procedures

The experiments were carried out in a rotating photoreactor, which has been used widely in photochemical experiments [33]. Water samples were placed into the sample quartz tubes, and the 500 W xenon lamps used to provide simulative solar light were placed into a quartz-tube cold well, which is located at the central axis. The distance from the sample quartz tubes to the axis is approximately 5 cm and the average light intensity on the surface of the sample quartz tubes was 130 mW/cm^2 according to a broadband power meter (Newport Corporation, Beijing, China). The sample quartz tubes rotate around the central axis, driven by a motor, while the water samples are simultaneously stirred by a magnetic rotor inside the quartz tube to ensure that reaction conditions are uniformly suspended. Experiments were carried out changing the following variables: (a) initial NO_3^- concentration, (b) initial substrate concentration, (c) initial pH, (d) initial humic acid (HA) concentration, and (e) initial Fe^{3+} concentration. Most of the experiments were performed at an initial concentration of 5 mg/L methyl parathion. Lower and higher concentrations were used to study the behavior of methyl parathion photodecomposition at different initial concentrations.

ANALYSIS

HPLC Analysis of Methyl Parathion

The quantification of the methyl parathion was performed with an Agilent 1200 Series quaternary liquid chromatograph (LC) equipped with a photodiode array detector (PDA) set at 275 nm. A C18 Discovery HS (Supelco) column (4.6 mm × 250 mm, 5 μm) was utilized as a stationary phase, while the mobile phase was a mixture of 30% (v/v) methyl alcohol and Milli-Q water in a 30:70 ratio. The analysis was conducted under isocratic conditions and methyl parathion was eluted at approximately 8.5 min. The flow rate was set at 1 mL/min and the injection volume was 20 μL. The temperature of the column was set at 30°C.

IC Analysis of Orthophosphate

Inorganic ions were analyzed by ionic chromatography from Dionex (ICS-1100) by using an eluent composed of 0.0045 mol/L of sodium carbonate and 0.0014 mol/L of sodium bicarbonate at the flow rate of 1.0 mL min^{-1} and injection volume of 25 μL. The temperature of the column was set at 30°C and the curb harmonic was 25 mA.

GC-MS Analysis of Methyl Parathion and Its Photoproducts

The methyl parathion and photodecomposition products were analyzed on a Shimadzu QP 5000 instrument, equipped with a DB 5-MS column of 30 cm length and an inner diameter of 0.25, coated with 5% phenyl 95% methyl polysiloxane. Separation of the by-products was conducted under the following chromatographic conditions: injector temperature 240°C, oven temperature program 55°C ramped at 5°C/min to 200°C followed by another ramp of 1°C/min to 210°C, held for 2 min and finally, to 270°C at 20°C/min (held for 3 min). Helium was used as the carrier gas at a flow of 1 mL min^{-1}. The temperatures of the ion source and the interface were set at 240 and 290°C, respectively. The MS operated in electron ionization mode with a potential of 70 eV and the spectra were obtained at a scan range from m/z 50∼450 (full scan mode). The scan time was 47 min and 1.0 μL injections were made.

Identification of •OH in NO_3^-/Solar System

The hydroxyl radical plays a critical role in the oxidative photodecomposition of organic compounds. To detect the production of •OH radicals in the process of methyl parathion decomposition in a NO_3^-/solar system, the following method was used: 10^{-3} M of NO_3^- was added to a 50 mL aqueous solution containing 1.0×10^{-4} M terephthalic acid and 4×10^{-4} M NaOH in a beaker and then transferred into solar irradiation. Next, 5 mL of the solution was collected per hour. Photoluminescence spectra of the 2-hydroxyterephthalic acid produced by the reaction between terephthalic acid and photogenerated hydroxyl radicals were recorded on a Shimadzu RF-5301 PC spectrometer using Excitation wavelength of 315 nm (EX = 315 nm), and scanning light wavelength of 350–600 nm (EM = 350–600 nm).

RESULTS AND DISCUSSION

Photodecomposition of Methyl Parathion by NO_3^-

To reveal the influence of NO_3^- photochemical activity on the transformation of organic phosphorus under a natural aquatic environment, the photodecomposition of methyl parathion by NO_3^- was performed under solar irradiation. The photodecomposition of methyl parathion was carried out under NO_3^- systems of different concentrations to probe the effect of NO_3^- concentration on the photodecomposition efficiency. The results show that the disappearance rate of methyl parathion in the presence of NO_3^- increased with the increase of nitrite concentration with the passage of irradiation time. The concrete condition, as shown in Figure 1, indicated that the photodecomposition of methyl parathion in a NO_3^-/solar system followed pseudo first-order kinetics. The pseudo first-order photodecomposition rate constant and half-life of methyl parathion by NO_3^- can be calculated per Eqs. (3) and (4) [34] as

$$\ln \frac{C}{C_0} = -kt \quad (3)$$

$$t_{1/2} = \frac{\ln 2}{k} \quad (4)$$

Where C_0 represents the methyl parathion concentration at time 0, C represents the methyl parathion concentration at time t, k is the pseudo-first-order rate constant (h^{-1}) and $t_{1/2}$ is the half-life, which have been summarized in Table 1. The rate constants of methyl parathion photodecompositions by

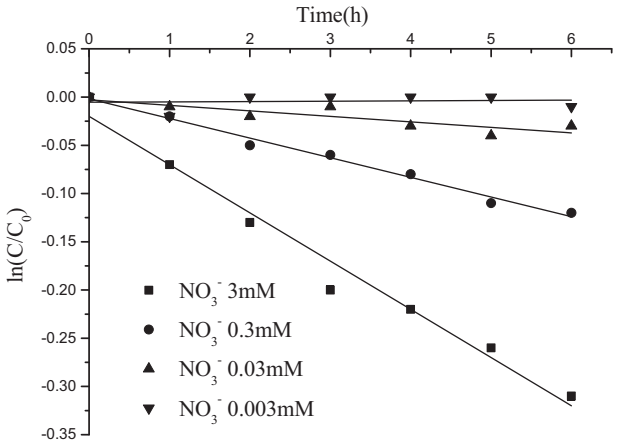

Figure 1. Effect of NO_3^- concentration on the phototransformationof methyl-parathion under simulated sunlight irradiation.

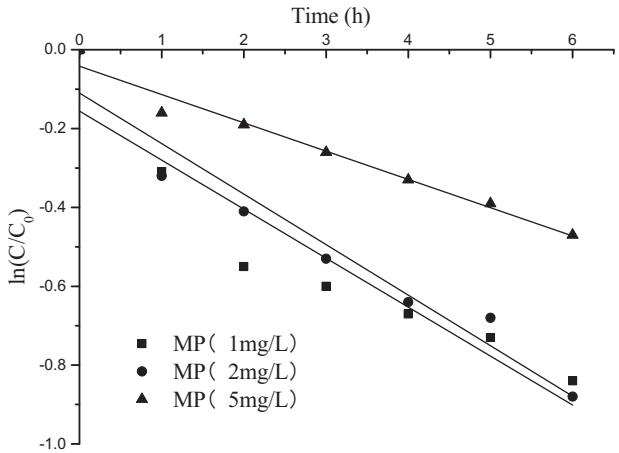

Figure 2. Effect of initial concentrationon methyl parathionphototransformation in thepresence of NO_3^- ($[NO_3^-] = 3$ mM).

Table 1. Pseudo-first-order rate constant, *k* and half-life for sunlight phototransformation of methyl-parathion (5 mg/L) at different NO_3^- concentrations.

NO_3^- (mM)	k (h^{-1})	$t_{1/2}$ (h)	R^2
0.003	0.0004	–	0.9600
0.03	0.0057	121.39	0.9714
0.3	0.0204	30.06	0.9858
3	0.0500	13.86	0.9732

Table 2. Pseudo-first-order rate constant, *k* and half-life for sunlight phototransformation at different methyl parathion initial concentrations.

MP (mg/L)	k (h^{-1})	$t_{1/2}$ (h)	R^2
1	0.1282	5.58	0.8586
2	0.1243	5.41	0.9329
5	0.0718	9.66	0.9672

NO_3^- are 0.0500, 0.0204, 0.0057, and 0.0004 h^{-1} for NO_3^- concentrations of 3 mM, 0.3 mM, 0.03 mM, and 0.003 mM, respectively. Nitrate ion absorption is at wavelengths of 200 nm and 300 nm, so the simulated solar conditions cause absorption of photons at 300 nm, producing active species [35]. Reactions of methyl parathion with active species can occur and promote photodecomposition.

Effect of Initial Concentrations

Figure 2 shows that the efficiency of methyl parathion photodecomposition by NO_3^- is related to the initial concentration of methyl parathion. The photodecomposition rate of methyl parathion increased with a decrease of initial concentration in the range of 1∼5 mg L^{-1}; this result was similar to those of previous reports [28]. The photodecomposition rate of methyl parathion was 0.1282, 0.1243, and 0.0718 h^{-1} for the initial concentrations of methyl parathion of 1, 2, 5 mg L^{-1} (Seen in Table 2), respectively. When the concentration of methyl parathion is 1.0 mg L^{-1}, 63.2% of the methyl parathion could be degraded by NO_3^- after 6 h of irradiation. This result can be explained by considering the competition to absorb the limited quantity of available photons by methyl parathion. Because the initial concentration of methyl parathion increased, but the number of available active species from the NO_3^- photochemical activity did not change, the number of active species available for per molecule of methyl parathion decreased, so the photodecomposition rate of methyl parathion decreased.

Effect of Initial pH Values

The solution pH can also have a pronounced effect on the speciation and reactivity of NO_3^- oxidative processes, as well as the protonation of organic functional groups. The effects of solution pH on the methyl parathion photodecomposition were investigated at 3 mM NO_3^- and 5 mg L^{-1} methyl parathion under solar irradiation. The solution pH was adjusted from 6 to 9 by the addition of 0.1 M HCl or 0.1 M NaOH. The photodecomposition of methyl parathion by NO_3^- as a function of irradiation time at different solution pH is illustrated in Figure 3. The observed photodecomposition of methyl parathion is strongly dependent on pH in a NO_3^-/solar system and the photodecomposition rate was decreasing with increasing pH. The first-order rate constants shown in Table 3 are 0.063, 0.0625, 0.0610, 0.0535, and 0.0457 h^{-1} for pH of 6, 7, 8, and 9, respectively. This result indicates that the photodecomposition rate of methyl parathion in the NO_3^-/solar system was inhibited with increasing

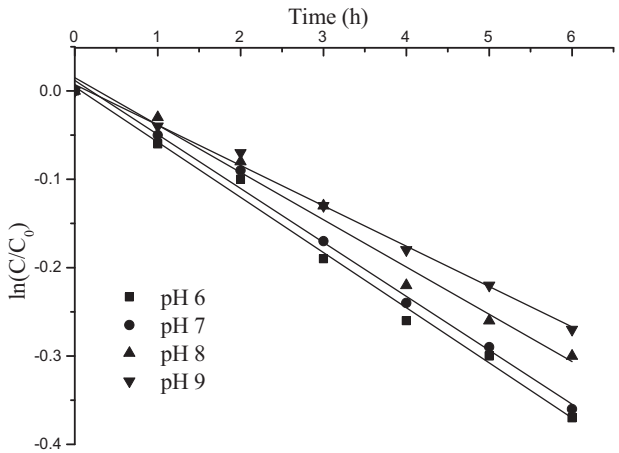

Figure 3. Kinetics of methyl parathion photo-induced transformation in the presence of $NO_3^-$with various pH values ($[NO_3^-] = 3$ mM, [MP] = 5 mg/L).

Table 3. Influence of pH on sunlight phototransformation at different methyl parathion in the presence of NO_3^-.

pH	k (h^{-1})	$t_{1/2}$ (h)	R^2
6	0.0625	11.09	0.9916
7	0.0610	11.35	0.9925
8	0.0535	12.94	0.9821
9	0.0457	15.16	0.9942

Table 4. Influence of humic acid on sunlight phototransformation at different methyl parathion in the presence of NO_3^-.

HA (mg/L)	k (h^{-1})	$t_{1/2}$ (h)	R^2
0	0.0860	8.06	0.9664
2	0.0739	9.38	0.9804
4	0.0557	12.44	0.9344
6	0.0621	11.16	0.9433

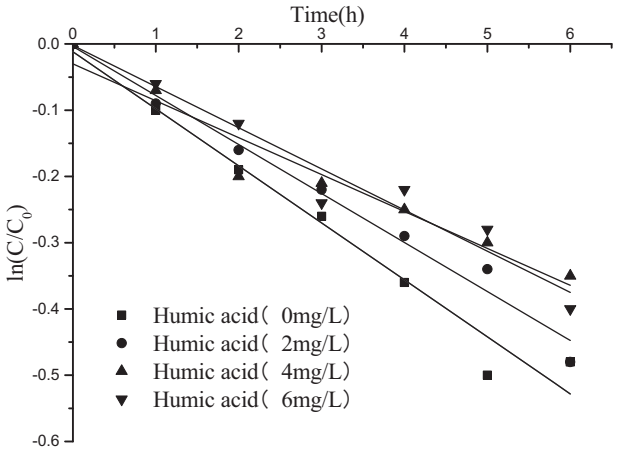

Figure 4. Effect ofhumic acidon methyl parathionphototransformation in thepresence of NO_3^- ($[NO_3^-] = 3$ mM, [MP] = 5 mg/L).

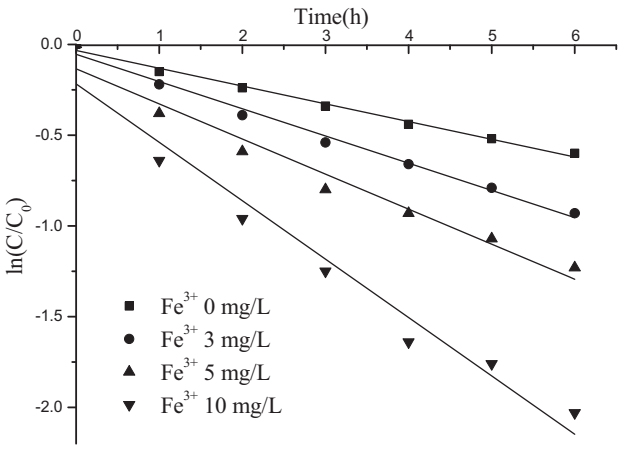

Figure 5. Effect of Fe^{3+} on methyl parathionphototransformation in the presence of NO_3^- ($[NO_3^-] = 3$ mM, [MP] = 5 mg/L).

pH. The cause of this result is that in an acidic medium, NO_2^- is in its acidic form (HNO_2, pKa =3.37) and becomes more reactive because of a higher absorption and a higher quantum yield of the •OH. So, the decrease in pH accelerated the kinetics induced by nitrites.

Effect of Humic Acid

Humic acids (HA) are the largest fraction of dissolved organic matter in the aquatic environment. This substance contains large amounts of oxygen-containing functional groups including phenolic hydroxyl and carboxyl groups. It can reach an active state through absorption of solar radiation at wavelengths between 300 ~ 500 nm; hence, the generation of free radicals (e.g., hydroxyl radicals, peroxyl radicals and singlet oxygen) that have a strong ability for oxidation on organic contaminants. This finding indicates that the humic Acid plays an important role in the photochemical processes that occur in surface waters [36].It has been reported that the existence of HA could accelerate the photodecomposition of organic matter under irradiation due to the photosensitization of HA [37,38]. In the presence of both HA and nitrite ions (10^{-2} M), methyl parathion disappeared more slowly than in the presence of nitrite alone at pH 7 (Figure 4). This phenomenon indicated that the photodecomposition rate of methyl parathion decreased with the increase of HA concentration. The k and $t^{1/2}$ values are reported in Table 4. The inhibition effect of HA to methyl parathion photolysis in a NO_3^-/solar system is observed mainly because the HA possesses a scavenging action to hydroxyl radicals [36].

Effect of Iron Ion Concentration

Iron ions, which usually exist in aqueous solutions in the form of $Fe(OH)^{2+}$ complexes, are widely distributed in natural waters and play a two-fold role in the NO_3^-/solar system. The $Fe(OH)^{2+}$ can be divided into Fe^{2+} and •OH under conditions of solar irradiation [39]. At the same time, nitrates are an efficient electron acceptor and excessively consume UV light intensity in the photoreactor. In addition, the generated Fe^{2+} will be an efficient •OH scavenger. The general reaction can be expressed as follows [40,41]:

$$Fe^{3+} + H_2O \rightarrow Fe(OH)^{2+} \quad (5)$$

$$Fe(OH)^{2+} + h\nu \rightarrow Fe^{2+} + \bullet OH \quad (6)$$

$$Fe^{2+} + \bullet OH \rightarrow Fe^{3+} + OH^-$$

The effect of Fe^{3+} concentration on the photodecomposition of methyl parathion in a NO_3^-/solar system is shown in Figure 5. Obviously, Fe^{3+} acted mainly as an •OH generator rather than as solar light filter in this study. The results indicated that compared to the NO_3^-/solar system, the photodegradation rate of methyl parathion was higher in the NO_3^-/solar system with Fe (III) added (Seen in Table 5). This result is consistent with previous studies on the photodecomposition of iopamidol by the Fe (III)/solar system [42]. Higher Fe (III) concentrations could result in the formation of more reactive oxygen species (ROS), but high concentrations can also lead to accelerating the photodecomposition of methyl parathion.

Determination of •OH in the NO_3^-/Solar System

To reveal the active species involved in the photoinduced decomposition of methyl parathion in the presence of a NO_3^-/solar system, the formation of hydroxyl radicals (•OH) in the presence of NO_3^- under simulated solar irradiation was identified by the PL technique using terephthalic acid as a probe molecule, which readily reacts with •OH to

produce a highly fluorescent product, that is, 2-hydroxyterephthalic acid [43]. The PL intensity of 2-hydroxyterephtalic acid at 425 nm is proportional to the amount of •OH produced in the degradation system in the presence of NO_3^-. Figure 6 presents the time course of fluorescence spectral changes with excitation at 315 nm under simulated solar irradiation in the presence of NO_3^-. It could be found that the PL intensity increased with the increase of irradiation time in the NO_3^-/solar system, which means the yield of •OH radicals have impressive promotion.

The active species of •OH were further verified by examining the effects of selected radical scavengers on this process. Methanol was tested as scavengers of •OH radicals to evaluate the role of •OH radicals in the oxidation of methyl parathion by NO_3^-. Figure 7 compares the total concentration of methyl parathion degradation after 6 h of irradiation in the presence of methanol. The photodegradation of methyl parathion was inhibited significantly with the addition of methanol. This result indicates that the generation of •OH radicals are the main reason for the photodegradation of methyl parathion in the NO_3^-/solar system.

Photodecomposition Pathways of Methyl Parathion by NO_3^-

GC–MS analysis was used to identify the intermediates formed during the photocatalytic degradation of methyl parathion. The fixed concentration of 100 mg/L methyl parathion was used for the intermediates analyses. Solar irradiation was stopped at 2 h during methyl parathion photodecomposition by NO_3^-. GC–MS analysis of solvent-extracted samples during the middle of reaction showed many intermediates peaks for methyl parathion (Figure 8). Peaks at 28.84, 26.69, and 14.57 min have been identified as methyl parathion, methyl paraoxon and 4-nitrophenol.

Ion chromatography was used to analyze the formation of inorganic anions during photo-induced photodecomposition of methyl parathion in the presence of NO_3^-. The experiment was carried out with 3 mM NO_3^-, and 5 mg L^{-1} methyl parathion under solar irradiation stopped at 2 h during methyl parathion photodecomposition by NO_3^-. As shown in Figure 9, the peak of orthophosphate was screened by the higher concentration of NO_3^-. Figure 9 shows that the concentration of orthophosphate increased with the increase of radiation intensity in the presence of NO_3^-, suggesting that organic phosphorus could be transformed into orthophosphate by the NO_3^- for its photochemical activity.

Based on the qualitative and quantitative analysis of organic and inorganic byproducts, the photodecomposition pathways of methyl parathion to orthophosphate by NO_3^- were proposed for •OH reactions, shown in Scheme 1. Degradation of MP starts with desulphurization, generating sulphate ions and methyl paraoxon. The oxidation of methyl

Table 5. Influence of Fe^{3+} on sunlight phototransformation at different methyl parathion in the presence of NO_3^-.

Fe^{3+} (mg/L)	k (h^{-1})	$t_{1/2}$ (h)	R^2
0	0.0978	7.08	0.9893
3	0.1500	4.62	0.9876
5	0.1932	3.59	0.9574
10	0.3218	2.15	0.9567

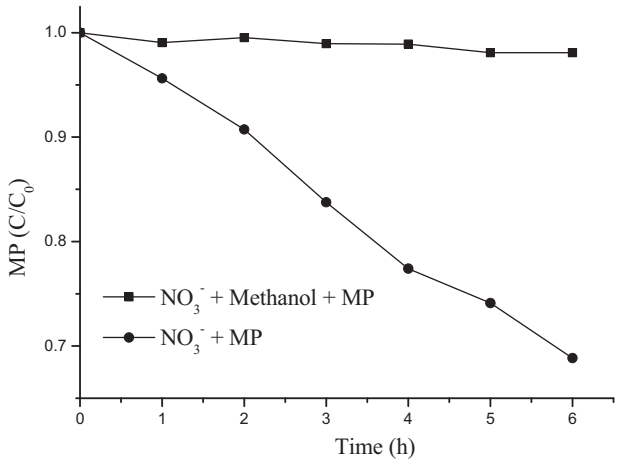

Figure 7. Significant suppression of the methyl parathion photo-induced transformation by several •OH radical scavengingagents ($[NO_3^-] = 3$ mM, [MP] = 5 mg/L).

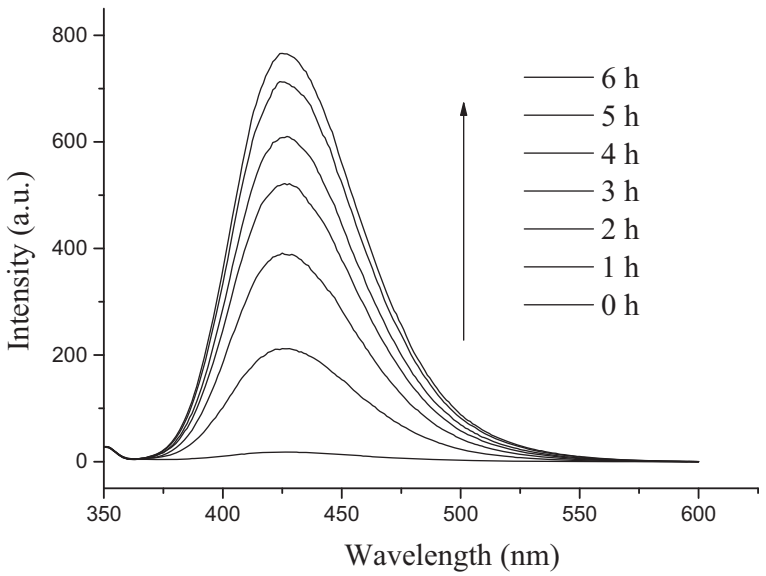

Figure 6. Fluorescence spectral changes of terephthalic acidin the presence of NO_3^- ($[NO_3^-] = 3$ mM).

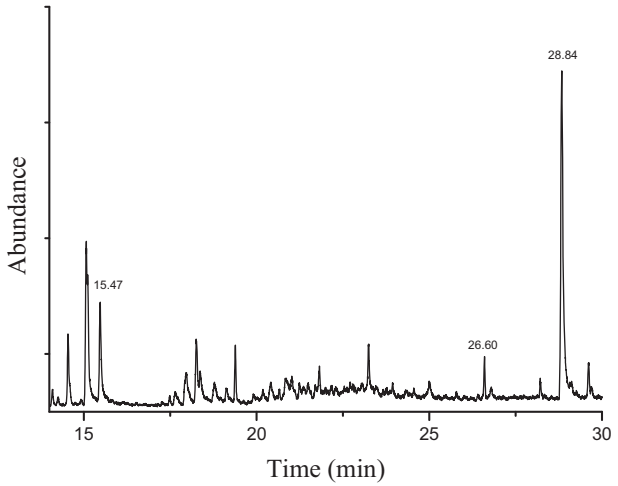

Figure 8. GC–MS analysis of commercial grade methyl parathion under sunlight radiationin the presence of NO_3^- (sample was collected at 2 h of the reaction for 100 mg/L of methyl parathion).

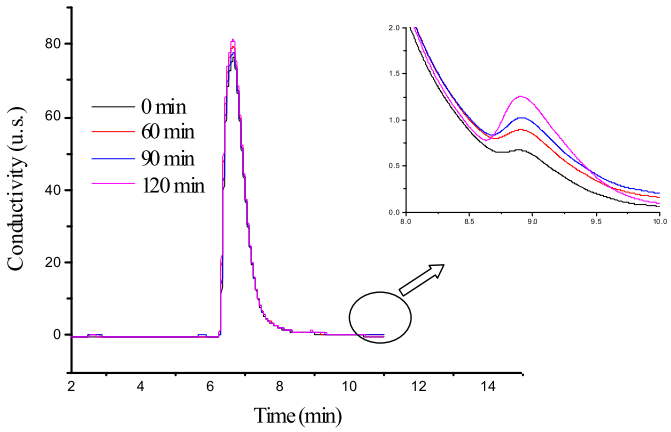

Figure 9. Formationof inorganic anions during the photo-induced transformation of methyl parathion in thepresence of NO_3^- (Insert is the peak of orthophosphate). [Color figure can be viewed at **wileyonlinelibrary.com**]

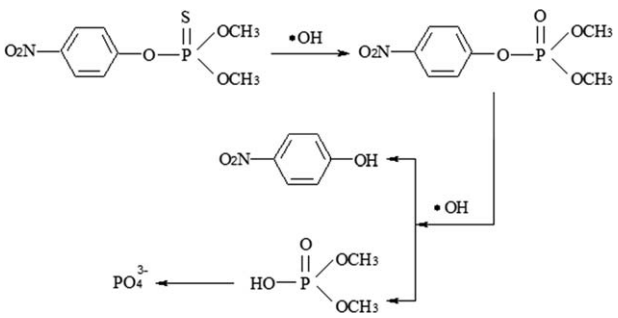

Scheme 1. Proposed reaction mechanism for the methyl parathion photo-induced transformation to orthophosphate.

paraoxon by hydrogen atom abstraction reactions leads to the formation of 4-nitrophenol and dimethyl phosphate. Successive additional reactions of hydroxyl radicals on the dimethyl phosphate lead to the formation of orthophosphate.

CONCLUSIONS

The influence of photochemical activity of NO_3^- on the photodecomposition of methyl parathion was investigated in this work. Methyl parathion can be degraded effectively in the NO_3^-/solar system, and the photodegradation rate of methyl parathion increased with increasing nitrite concentration. Moreover, the photodegradation rate of methyl parathion in the NO_3^-/solar was affected by varying environmental parameters, including inducer and substrate concentrations, pH, and the concentration of HA and Fe^{3+}. Using terephthalic acid as a trapping molecule determined that the production of •OH radicals in the NO_3^-/solar system and the concentration of NO_3^- was critical and correlates to the formation of •OH through the process of irradiation. Reaction products and pathways were elucidated based on the qualitative and quantitative analysis of organic and inorganic byproducts. For the main oxidation process, the methyl parathion was oxidized into paraoxon and then further oxidized into 4-nitrophenol and orthophosphate by •OH radicals. Furthermore, all of these results can also be applied to the organic phosphorus that is converted into orthophosphate in the aquatic environment in the NO_3^-/solar system.

ACKNOWLEDGMENTS

This research was supported by the National Natural Science Foundation of China (41230748, 41401547), Fundamental Research Funds for the Central Universities (2662016PY061), the Fok Ying-Tong Education Foundation, China (151078), the China Postdoctoral Science Foundation (2013M540619, 2015T80855) and the Open Project of State Key Laboratory of Freshwater Ecology and Biotechnology (2015FB04).

LITERATURE CITED

1. Conley, D.J., Paerl, H.W., Howarth, R.W., Boesch, D.F., Seitzinger, S.P., Havens, K.E., Lancelot, C., & Likens, G.E. (2009). Controlling eutrophication: Nitrogen and phosphorus, Science, 20, 1014–1015.
2. Meinikmann, K., Hupfer, M., & Lewandowski, J. (2015). Phosphorus in groundwater discharge – A potential source for lake eutrophication, Journal of Hydrology, 524, 214–226.
3. Qin, C., Liu, H., Liu, L., Smith, S., Sedlak, D.L., & Gu, A.Z. (2015). Bioavailability and characterization of dissolved organic nitrogen and dissolved organic phosphorus in wastewater effluents, Science of the Total Environment, 511, 47–53.
4. Zhu, Y., Wu, F., He, Z., Giesy, J.P., Feng, W., Mu, Y., Feng, C., Zhao, X., Liao, H., & Tang, Z. (2015). Influence of natural organic matter on the bioavailability and preservation of organic phosphorus in lake sediments, Chemical Geology, 397, 51–60.
5. Gardolinski, P.C.F.C., Worsfold, P.J., & McKelvie, I.D. (2004). Seawater induced release and transformation of organic and inorganic phosphorus from river sediments, Water Research, 38, 688–692.
6. Xu, D., Ding, S., Li, B., Bai, X., Fan, C., & Zhang, C. (2013). Speciation of organic phosphorus in a sediment profile of Lake Taihu I: Chemical forms and their transformation, Journal of Environmental Sciences, 25, 637–644.
7. Jin, X., Jiang, Y., Yao, Y., Li, L., & Wu, F.C. (2006). Effects of light and oxygen on the uptake and distribution of phosphorus at the sediment–water interface, Science of the Total Environment, 357, 231–236.
8. Tallberg, P., Treguer, P., Beucher, C., & Corvaisier, R. (2008). Potentially mobile pools of phosphorus and silicon in sediment from the Bay of Brest: Interactions and

implications for phosphorus dynamics, Estuarine Coastal and Shelf Science, 76, 85–94.
9. Zee, C.V.D., Roevros, N., & Chou, L. (2007). Phosphorus speciation, transformation and retention in the Scheldt estuary (Belgium/The Netherlands) from the freshwater tidal limits to the North Sea, Marine Chemistry, 106, 76–91.
10. Wang, S., Jin, X., Zhao, H., Zhou, X., & Wu, F. (2008). Effects of organic matter on phosphorus release kinetics in different trophic lake sediments and application of transition state theory, Journal of Environmental Management, 88, 845–852.
11. Lake, B.A., Coolidge, K.M., Norton, S.A., & Amirbahman, A. (2007). Factors contributing to the internal loading of phosphorus from anoxic sediments in six Maine, USA, lakes, Science of the Total Environment, 373, 534–541.
12. Turner, B.L., Frossard, F., & Baldwin, D. (2005). Organic phosphorus in the environment, CABI Publishing, Cambridge.
13. Dyhrman, S., Chappell, P., Haley, S., Moffett, J., Orchard, E., Waterbury, J., & Webb, E. (2006). Phosphonate utilization by the globally important marine diazotroph Trichodesmium, Nature, 439, 68–71.
14. Stets, E.G., & Cotner, J.B. (2008). The influence of dissolved organic carbon on bacterial phosphorus uptake and bacteria-phytoplankton dynamics in two Minnesota lakes, Limnology and Oceanography, 53, 137–147.
15. Nowack, B. (2003). Environmental chemistry of phosphonates, Water Research, 37, 2533–2546.
16. Chen, Y., Wu, F., Lin, Y., Deng, N., Bazhin, N., & Glebov, E. (2007). Photodegradation of glyphosate in the ferrioxalate system, Journal of Hazardous Materials, 148, 360–365.
17. Sandy, E.H., Blake, R.E., Chang, S.J., Jun, Y., & Yu, C. (2013). Oxygen isotope signature of UV degradation of glyphosate and phosphonoacetate: Tracing sources and cycling of phosphonates, Journal of Hazardous Materials, 260, 947–954.
18. Southwell, M.W., Kieber, R.J., Mead, R.N., Avery, G.B., & Skrabal, S.A. (2010). Effects of sunlight on the production of dissolved organic and inorganic nutrients from resuspended sediments, Biogeochemistry, 98, 115–126.
19. Sindelar, H.R., Lloyd, J., Brown, M.T., & Boyer, T.H. (2015). Transformation of dissolved organic phosphorus to phosphate using UV/H_2O_2, Environmental Progress Sustainable Energy, 35, 680–691.
20. Southwell, M.W., Mead, R.N., Luquire, C.M., Barbera, A., Avery, G.B., Kieber, R.J., & Skrabal, S.A. (2011). Influence of organic matter source and diagenetic state on photochemical release of dissolved organic matter and nutrients from resuspendable estuarine sediments, Marine Chemistry, 126, 114–119.
21. Mack, J., & Bolton, J.R. (1999). Photochemistry of nitrite and nitrate in aqueous solution: a review, Journal of Photochemistry and Photobiology A: Chemistry, 128, 1–13.
22. Malouki, M.A., Lavédrine, B., & Richard, C. (2005). Phototransformation of methabenthiazuron in the presence of nitrate and nitrite ions, Chemosphere, 60, 1523–1529.
23. Matykiewiczová, N., Kurková, R., Klánová, J., & Klán, P. (2007). Photochemically induced nitration and hydroxylation of organic aromatic compounds in the presence of nitrate or nitrite in ice, Journal of Photochemistry and Photobiology A: Chemistry, 187, 24–32.
24. Boucheloukh, H., Sehili, T., Kouachi, N., & Djebbar, K. (2012). Kinetic and analytical study of the photo-induced degradation of monuron by nitrates and nitrites under irradiation or in the dark, Photochemical Photobiological Sciences, 11, 1339–1345.
25. Liu, G., Gong, L., Zhou, Y., Zhu, D., Cao, X., & Song, C. (2015). NO_3^-/NO_2^- photosensitized degradation of phenol under simulated sunlight, Fresenius Environmental Bulletin, 24, 664–669.
26. Calza, P., Vione, D., Novelli, A., Pelizzetti, E., & Minero, C. (2012). The role of nitrite and nitrate ions as photosensitizers in the phototransformation of phenolic compounds in seawater, Science of the Total Environment, 439, 67–75.
27. Wang, G., Liu, G., Liu, H., Zhang, N., & Wang, Y. (2012). Photodegradation of salicylic acid in aquatic environment: Effect of different forms of nitrogen, Science of the Total Environment, 435–436, 573–577.
28. Passananti, M., Temussi, F., Iesce, M.R., Mailhot, G., & Brigante, M. (2013). The impact of the hydroxyl radical photochemical sources on the rivastigmine drug transformation in mimic and natural waters, Water Research, 47, 5422–5430.
29. Warneck, P., & Wurzinger, C. (1988). Product quantum yields for the 305 nm photodecomposition of NO_3^- in aqueous solution, Journal of Physical Chemistry C, 92, 6278–6283.
30. Rastogi, S.K., Singh, V.K., Kesavachandran Jyoti, C., Siddiqui, M.K.J., Mathur, N., & Bharti, R.S. (2008). Monitoring of plasma butyrylcholinesterase activity and haematological parameters in pesticide sprayers, Journal of Occupational and Environmental Medicine, 12, 29–32.
31. Oliva, J., Barba, A., Vela, N., Melendreras, F., & Navarro, S.J. (2000). Multiresidue method for the rapid determination of organophosphorus insecticides in grapes: Must and wine, Journal of Chromatography A, 882, 213–220.
32. Pappas, C.J., Kyriakidis, N.B., & Athanasopoulos, P.E. (1998). Journal of AOAC International, 82, 359–363.
33. Nélieu, S., Shankar, M.V., Kerhoas, L., & Einhorn, J. (2008). Phototransformation of monuron induced by nitrate and nitrite ions in water: Contribution of photonitration, Journal of Photochemistry and Photobiology A: Chemistry, 193, 1–9.
34. Xie, H., Zheng, Q., Wang, S., Ma, C., Gao, G., Bing, N., & Sun, Z. (2014). Capture of phosphates in surface water by TiO_2 nanoparticles underUV irradiation, Particuology, 14, 98–102.
35. Shankar, M.V., Nélieu, S., Kerhoas, L., & Einhorn, J. (2007). Photo-induced degradation of diuron in aqueous solution by nitrites and nitrates: Kinetics and pathways, Chemosphere, 66, 767–774.
36. Chowdhury, R.R., Charpentier, P.A., & Ray, M.B. (2011). Photodegradation of 17-βestradiol in aquatic solution under solar irradiation: Kinetics and influencing water parameters, J. Photochemical Photobiological Sciences, 219, 67–75.
37. Prosen, H., & Kralj, L.Z. (2005). Evaluation of photolysis and hydrolysis of atrazine and its first degradation products in the presence of humic acids, Environmental Pollution, 133, 517–529.
38. Kohn, T., & Nelson, K.L. (2007). Sunlight-mediated inactivation of MS2 coliphage via exogenous singlet oxygen produced by sensitizers in natural waters, Environmental Science Technology, 41, 192–197.
39. Kohn, T., Grandbois, M., McNeill, K., & Nelson, K.L. (2007). Association with natural organic matter enhances the sunlight-mediated inactivation of MS2 coliphage by singlet oxygen, Environmental Science Technology, 41, 4626–4632.
40. Shah, N.S., He, X., Khan, J.A., Khan, H.M., Boccelli, D.L., & Dionysiou, D.D. (2015). Comparative studies of various iron-mediated oxidative systems for the photochemical degradation of endosulfan in aqueous solution, Journal

of Photochemistry and Photobiology A: Chemistry, 306, 80–86.
41. Shah, N.S., Khan, J.A., Nawaz, S., Ismail, M., Khan, K., & Khan, H.M. (2015). Kinetic and mechanism investigation on the gamma irradiation induced degradation of endosulfan sulfate, Chemosphere, 121, 18–25.
42. Zhao, C., Arroyo-Mora, L.E., DeCaprio, A.P., Sharma, V.K., Dionysiou, D.D., & ÓShea, K.E. (2014). Reductive and oxidative degradation of iopamidol, iodinated X-ray contrast media, by Fe(III)-oxalate under UV and visible light treatment, Water Research, 67, 144–153.
43. Charbouillot, T., Brigante, M., Mailhot, G., Maddigapu, P.R., Minero, C., & Vione, D. (2011). Performance and selectivity of the terephthalic acid probe for •OH as a function of temperature, pH and composition of atmospherically relevant aqueous media, Journal of Photochemistry and Photobiology a: Chemistry, 222, 70–76.